Zero Dimensional Polariton Laser in a Sub-Wavelength Grating Based Vertical Microcavity

Bo Zhang, Zhaorong Wang and Hui Deng

Department of Physics, University of Michigan, Ann Arbor, Michigan, 48109

Sebastian Brodbeck, Christian Schneider, Martin Kamp and Sven Höfling

Technische Physik, Physikalisches Institut and Wilhelm Conrad Röntgen Research Center for Complex Material Systems, Universität Würzburg, D-97074 Würzburg, Germany

Abstract

Semiconductor microcavity exciton-polaritons have emerged as a unique, open system that exhibits manybody quantum orders without thermal equilibrium. Hallmarks of non-equilibrium condensation and superfluidity have been widely observed in 2D. Progress beyond 2D condensation physics, however, has been hindered by the limited means to confine the polaritons and to couple multiple polariton systems in conventional microcavities. Here we demonstrate the control of the dimensionality and polarization of the polaritons by design using a hybrid cavity made of a single-layer sub-wavelength grating mirror and a distributed Bragg reflector. Three-dimensional confinement of polaritons was achieved and single-mode polariton lasing was observed at a predefined polarization. Incorporation of a designable slab mirror into the conventional vertical cavity, when operating in the strong-coupling regime, enables confinement, control and coupling of polariton gasses in a scalable fashion. It may open a door to experimental implementation of polariton-based quantum photonic devices and coupled cavity quantum electrodynamics systems.

Exciton-polaritons are formed via strong coupling between the excitons and photons. Due to the excitonic component, polaritons are massive, weakly interacting quasi-particles that feature strong nonlinearity and rich manybody physics [1]. Due to the mixing with the photon, polaritons have an effective mass 10^{-8} of the Hydrogen atom mass, and they are relatively insensitive to disorders or localization potentials in the active media. Hence polaritons exhibit quantum coherence over macroscopic scales at high critical temperatures. Polaritons in quantum-well (QW) microcavities [2] couple out of the cavity at a fixed rate while conserving the energy and in-plane wavenumber, providing direct experimental access unavailable in typical manybody quantum systems. These features make QW-microcavity polaritons (which we will abbreviate as polaritons in this paper) uniquely suited for non-equilibrium manybody physics studies [3–5]. Hallmarks of non-equilibrium condensation and superfluidity have been widely observed in isolated two-dimensional polariton systems (Ref. [6] and references therein). These foundational work has inspired theoretical schemes for polariton-based quantum circuits [7–9], quantum light sources [10–13], and novel quantum phases [5]. The experimental implementation of these schemes require the creation and coupling of 0D and 1D polariton systems, which remain as a major experimental challenge with conventional microcavities.

To establish the polariton modes, a high quality λ-scale cavity is required to enhance the exciton-photon coupling and reduce the cavity photon decay rate. Conventionally it is achieved using two thick stacks of distributed Bragg reflectors (DBR), each DBR containing 20-40 pairs of $\lambda/4$ layers of alternating high and low refractive indices. The whole structure needs to be grown epitaxially using closely lattice-matched semiconductor alloys, which limits the choice of materials and availability of high quality samples. Furthermore, the thick DBRs make it difficult to confine or control the polaritons beyond the perturbative regime without suppressing strong coupling or polariton lasing. Many methods have been investigated to confine polaritons, including control of the excitons by mechanical strain and control of the optical modes by surface patterning [14, 15], by overgrowth over apertures inside the cavity [16, 17], and by direct etching of the vertical cavity into pillars and wires [18–24]. Only with the last approach, lasing of discrete lower dimensional polaritons has been achieved recently in two laboratories [22–25]. The deep etching process poses challenges to maintain the optical mode quality and to prevent exciton recombination at the etched sidewall, which may limit the scalability and wider applicability of the technique.

In this work, we circumvent the limitation of the thick vertical DBR by replacing it with a slab photonic crystal (PC) based on a sub-wavelength grating (SWG), creating a shorter, hybrid cavity structure, as shown in Fig. 1. Single-layer PC reflectors have been demonstrated in a variety of designs [26–28]. In particular, SWGs with high index-contrast have been successfully integrated in vertical surface emitting lasers (VCSELs) recently [29]. Here we achieve for the first time the strong-coupling regime using a SWG as the top mirror (Fig. 1(a)). Furthermore, we show that a finite-size grating creates an effective optical potential and enables three-dimensional confinement of the polaritons in a scalable fashion. Zero-dimensional polariton lasing was readily achieved, with a pre-defined linear polarization. The demonstrated hybrid cavity integrates a designable slab mirror with the QW-microcavity to allow flexible confinement, control, and coupling of polariton systems, while, at the same, leaving the QW excitons untouched and protected.

To fabricate the device, we first grew the planar structure by molecular beam epitaxy (MBE), consisting of an 80-nm thick $Al_{0.15}GaAs$ top layer on top of a sacrificial layer, followed by 2.5 pairs of top DBR of $Al_{0.15}GaAs/AlAs$, an AlAs $\lambda/2$ cavity layer, and 30-pairs of bottom DBR. There are 12 GaAs QWs distributed at the three central anti-nodes of the cavity. Square gratings of $5-8$ μm in length (Fig. 1(b)) were then created via electron-beam lithography, followed by a short plasma etching through the top layer and a selective wet etching to remove the sacrificial layer. The gratings have a period of ~ 520 nm and a duty cycle of $\sim 40\%$. It is optimized as a high reflectance mirror for light polarized along the grating bar direction (TE-polarization).

We characterized the properties of the cavity devices via real-space and Fourier space imaging. The sample was kept at 10-90 K in a continuous flow liquid-helium cryostat. A pulsed Ti-Sapphire laser at 740 nm was used as the excitation laser, with a 80 MHz repetition rate and 100 fs pulse duration. It is focused to a spot size of $\sim$2 μm in diameter on the device from the normal direction with an objective lens of a numerical aperture of 0.55. The photoluminescence signal was collected with the same objective lens and sent to a 0.5 m spectrometer and recorded by a nitrogen cooled charge coupled device (CCD). The spectrally resolved real space and Fourier space distributions were measured by selecting a strip across the center of the Fourier space and real space distributions using the spectrometer's entrance slit. The resolution of the measurements was limited by the CCD pixel size to ~ 0.3 /μ for Fourier space imaging and by the diffraction limit to ~ 0.4 μm for real space imaging.

The lateral size of the hybrid cavity is determined by the size of the high reflectance SWG. Outside the SWG, there is no cavity resonance and excitons are the eigen-excitations. Inside the SWG region, TE-polarized cavity modes strongly couple to excitons, leading to laterally confined TE-polarized polariton modes. TM-polarized excitons remain in the weak coupling regime.

We characterize the energies and mode-profile of a 7.5 μm×7.5 μm hybrid cavity by momentum-space and real-space imaging, as shown in Fig. 2(a)-(c). Figure 2(a) is the spectrally resolved k-space profile of the photoluminescence (PL) from outside the SWG, showing a flat exciton dispersion at the heavy hole exciton energy of E_{exc} =1.551 eV. Figure 2(b) shows the k-space image of TE-polarized PL from within the SWG. The exciton band disappeared; and discrete LP modes were observed below the exciton energy. A faint UP branch was also observed above the exciton energy. In the rotating wave approximation, the LP and UP energies are given by:

$$E_{UP,LP}(k) = \frac{1}{2}[E_{exc}(k) + E_{cav}(k) \pm \sqrt{(E_{exc}(k) - E_{cav}(k))^2 + 4\hbar^2\Omega^2}]. \quad (1)$$

Here k is the in-plane wavenumber, $E_{cav}(k)$ is the un-coupled cavity energy and 2Ω is the exciton-photon coupling strength, corresponding to the LP-UP splitting at the zero exciton-photon detuning. Using Eq. 1 and the measured $E_{exc}(0)$ =1.551 eV, $E_{LP}(k=0) = 1.543$ eV, and $E_{UP}(k=0) = 1.556$ eV, we obtain $E_{cav}(0) = 1.548$ eV and $2\hbar\Omega = 12$ meV.

The discrete modes of the LPs result from three-dimensional confinement due to the finite size of the SWG. Since there is not a sharp lateral boundary where the cavity mode disappear, we model the effective confinement potential as an infinite Harmonic potential phenomenologically. The calculated energies of the confined LP modes are indicated by the dashed lines in Fig. 2(b), and the confined cavity modes, by crosses. For comparison, the corresponding 2D dispersions of the LP, UP and cavity modes are also shown (solid lines). We have measured the same discrete modes in the spectrally resolved real-space images, as shown in Fig. 2(c). The four lowest LP modes are well confined within the SWG region, while higher excited states spread outside and form a continuous band. The variances of the k-space and x-space wavefunctions along the detected direction are $\Delta k = 0.85$ /μm and $\Delta x = 1.01$ μm. Their product is $\Delta x \times \Delta k = 0.86$. It is slightly larger than the uncertainty limit of 0.5, which may be due to the diffusion of the LPs.

The absorption spectra of the modes were obtained via reflectance measurements. The

spectrum measured normal to the sample (Fig. 2(d)) shows the three symmetric modes with the lowest mean in-plane wavenumber: the UP ground state, the LP ground state, and the LP second excited states. Other polariton states have too small a spectral weight to be measured in reflectance. When measured at 3.5° from the sample normal, the 1st excited state of LPs was also observed (Fig. 2(e)).

A further confirmation of the strong-coupling regime is the temperature tuning of the eigen-energies, as shown in Fig. 2(f). As the temperature increased, the LP and UP ground state energies red shifted and were measured via k-space PL. The exciton energy was measured directly in the planar region outside the SWG. The shift of the cavity photon energy was obtained from the shift of the 1st low-energy side minimum of the stopband. Anti-crossing of the LP and UP modes is evident. From the LP, exciton and cavity energies, we obtain the coupling strength $2\Omega(T)$ to be ~ 10 meV from 10 K to 80 K, showing that strong coupling persists to the liquid nitrogen temperature or higher.

The grating breaks the in-plane rotational symmetry. As a result, the SWG mirrors can have high polarization selectivity. We optimized our SWG to have high reflectance for the TE mode and low reflectance for the orthogonal TM mode. Correspondingly, the polaritons are TE polarized, while the TM polarized excitons remain in the weak coupling regime. Figure 3 shows the PL intensity vs. the angle of linear polarization for the LPs and excitons at $k \sim 0$ within the SWG region, normalized by the maximum intensity. We fit the data with $I = A\cos(\theta - \phi)^2 + B$, where the fitting parameters ϕ depends on the orientation of the device, A corresponds to linearly polarized light, and B corresponds to a non-polarized background. Correspondingly, the degrees of linear polarization is DOP$= \frac{I_{max}-I_{min}}{I_{max}+I_{min}} = \frac{A}{A+2B}$. We obtained $A_{LP} = 1.04 \pm 0.04$, $B_{LP} = 0.05 \pm 0.01$, $\phi_{LP} = 71° \pm 1°$, and DOP$= 91.9\%$ for the LPs, confirming that LPs are highly TE-polarized. For the excitons, we obtained $A_{exc} = 0.891 \pm 0.001$, $B_{exc} = 0.0081 \pm 0.0002$, $\phi_{exc} = 161° \pm 1° = \phi_{LP} + 90°$, and DOP$= 98.2\%$, showing that excitons are polarized orthogonal to the LPs. Such high degree of polarization selectivity has not been possible with conventional DBR-DBR cavities and is unique to the SWG-based cavity. It provides a complementary system for understanding the complex effects of the polarization degree of freedom in polariton dynamics and manybody physics [30].

Finally, we show that polariton lasing was achieved in the 0D hybrid cavity, as shown in Fig. 4. The energy separation between the discrete modes is larger than $k_B T \sim 0.8$ meV. As

a result, relaxation to the ground state is mainly through the nonlinear LP-LP scattering. As shown in Fig. 4(a), the ground state PL intensity I increases quadratically with the excitation density P at low P. Near the threshold density of $P =\sim 5$ KW/cm^2, I increases sharply with P, characteristic of the onset of lasing. Well above threshold, we recover the quadratic dependence. Accompanying the transition, a sharp decrease of the LP ground state linewidth was measured. The minimum linewidth of 0.24 meV may be limited mainly by the intensity fluctuation of the pulsed excitation laser [31]. The LP energy increased continuously with the excitation density due to exciton-exciton interactions. The blueshift shows a linear dependence below threshold, it is suppressed near threshold, and shows a logarithmic dependence above threshold [22, 32]. The discrete energy levels are maintained across the threshold and remain distinctly below the uncoupled cavity energy. The establishment of polariton lasing confirms the quality of the 0D-polariton system. This is the first demonstration of a polariton laser at *a priori* defined polarization, as well as a polariton condensate without a competing, nearly spin-degenerate mode.

In conclusion, we have demonstrated the first hybrid cavity incorporating a slab PC mirror, operating in the strong coupling regime. Three dimensional confinement of the polaritons was achieved by using a finite size SWG, leaving the QW excitons untouched. Polariton lasing in the ground state was readily observed, with similar spectral features as conventional DBR-DBR cavities [22]. .

Unique to the hybrid SWG-cavity, the LP is linearly polarized, while the orthogonally polarized exciton mode remains in the weak-coupling regime. The PL of the weakly-coupled TM excitons provides direct access to the exciton reservoir that has not been available in conventional cavity systems. Furthermore, it enables polarized polariton lasers [33–37] and simplifies quantum photonic devices based on single-spin polaritons [11–13, 38].

The integration of a slab PC mirror in a vertical cavity adds the flexibility to modify the photon modes, which, in the strong-coupling regime, enables control of the fundamental properties of polaritons by design, including the dimensionality and polarization, as demonstrated in this work. Moreover, the structure requires a shorter MBE growth time and can be fabricated via well established techniques for PCs in a typical nanofabrication facility. The demonstrated hybrid-cavity polariton system may provide a scalable architecture for the experimental implementation of coupled lattice cavity systems [5, 39].

We thank Lei Zhang for help with the initial design of the SWG mirror, and Jinhai

Chen for help with the initial experimental setup. ZB, ZW, and HD acknowledge the support by the National Science Foundation (NSF) under Awards DMR 1150593 and the Air Force Office of Scientific Research under Awards FA9550-12-1-0256. CS, SB, MK and SH acknowledge the support by the State of Bavaria, Germany. The fabrication of the SWG was performed in the Lurie Nanofabrication Facility (LNF) which is part of the NSF NNIN network.

[1] P. B. Littlewood, P. R. Eastham, J. M. J. Keeling, F. M. Marchetti, B. D. Simon, and M. H. Szymanska, J. Phys.: Cond. Matt. **16**, S3597 (2004), 35.

[2] C. Weisbuch, M. Nishioka, A. Ishikawa, and Y. Arakawa, Physical Review Letters **69**, 3314 (1992).

[3] J. Keeling, F. M. Marchetti, M. H. Szymaska, and P. B. Littlewood, Semiconductor Science and Technology **22**, R1 (2007).

[4] J. Keeling and N. G. Berloff, Nature **457**, 273 (2009), 7227.

[5] I. Carusotto and C. Ciuti, Reviews of Modern Physics **85**, 299 (2013).

[6] H. Deng, H. Haug, and Y. Yamamoto, Reviews of Modern Physics **82**, 1489 (2010).

[7] T. C. H. Liew, A. V. Kavokin, and I. A. Shelykh, Physical Review Letters **101**, 016402 (2008).

[8] I. A. Shelykh, R. Johne, D. D. Solnyshkov, and G. Malpuech, 1007.3665 (2010).

[9] T. C. H. Liew, A. V. Kavokin, T. Ostatnick, M. Kaliteevski, I. A. Shelykh, and R. A. Abram, Physical Review B **82**, 033302 (2010).

[10] A. Verger, C. Ciuti, and I. Carusotto, Physical Review B **73**, 193306 (2006).

[11] T. C. H. Liew and V. Savona, Physical Review A **85**, 050301 (2012).

[12] A. Majumdar, M. Bajcsy, A. Rundquist, and J. Vuckovic, Physical Review Letters **108**, 183601 (2012).

[13] T. C. H. Liew and V. Savona, New Journal of Physics **15**, 025015 (2013).

[14] M. M. de Lima, M. van der Poel, P. V. Santos, and J. M. Hvam, Physical Review Letters **97**, 045501 (2006).

[15] C. W. Lai, N. Y. Kim, S. Utsunomiya, G. Roumpos, H. Deng, M. D. Fraser, T. Byrnes, P. Recher, N. Kumada, T. Fujisawa, and Y. Yamamoto, Nature **450**, 529 (2007).

[16] O. E. Daif, A. Baas, T. Guillet, J. P. Brantut, R. I. Kaitouni, J. L. Staehli, F. Morier-Genoud,

and B. Deveaud, APPLIED PHYSICS LETTERS **88**, 061105 (2006), 6.

[17] K. Winkler, C. Schneider, J. Fischer, A. Rahimi-Iman, M. Amthor, A. Forchel, S. Reitzenstein, S. Höfling, and M. Kamp, Applied Physics Letters **102**, 041101 (2013).

[18] A. Tartakovskii, V. Kulakovskii, Y. Koval, T. Borzenko, A. Forchel, and J. Reithmaier, Journal of Experimental and Theoretical Physics **87**, 723 (1998), 4.

[19] T. Gutbrod, M. Bayer, A. Forchel, J. P. Reithmaier, T. L. Reinecke, S. Rudin, and P. A. Knipp, Physical Review B **57**, 9950 (1998), 16.

[20] G. Dasbach, M. Bayer, M. Schwab, and A. Forchel, Semiconductor Science and Technology **18**, S339 (2003).

[21] G. Dasbach, C. Diederichs, J. Tignon, C. Ciuti, P. Roussignol, C. Delalande, M. Bayer, and A. Forchel, Physical Review B **71**, 161308 (2005).

[22] D. Bajoni, P. Senellart, E. Wertz, I. Sagnes, A. Miard, A. Lemaitre, and J. Bloch, Physical Review Letters **100**, 047401 (2008).

[23] E. Wertz, L. Ferrier, D. D. Solnyshkov, R. Johne, D. Sanvitto, A. Lemaitre, I. Sagnes, R. Grousson, A. V. Kavokin, P. Senellart, G. Malpuech, and J. Bloch, Nat Phys **6**, 860 (2010).

[24] A. S. Brichkin, S. I. Novikov, A. V. Larionov, V. D. Kulakovskii, M. M. Glazov, C. Schneider, S. Höfling, M. Kamp, and A. Forchel, Physical Review B **84**, 195301 (2011).

[25] V. D. Kulakovskii, A. S. Brichkin, S. V. Novikov, C. Schneider, S. Höfling, M. Kamp, A. Forchel, and N. A. Gippius, Physical Review B **85**, 155322 (2012).

[26] C. F. R. Mateus, M. C. Y. Huang, Y. F. Deng, A. R. Neureuther, and C. J. Chang-Hasnain, Ieee Photonics Technology Letters **16**, 518 (2004), 2.

[27] I. W. Jung, S. Kim, and O. Solgaard, Journal of Microelectromechanical Systems **18**, 924 (2009).

[28] D. Fattal, J. Li, Z. Peng, M. Fiorentino, and R. G. Beausoleil, Nat Photon **4**, 466 (2010).

[29] M. C. Huang, Y. Zhou, and C. J. Chang-Hasnain, Nat Photon **1**, 119 (2007).

[30] I. A. Shelykh, A. V. Kavokin, Y. G. Rubo, T. C. H. Liew, and G. Malpuech, Semiconductor Science and Technology **25**, 013001 (2010).

[31] A. P. D. Love, D. N. Krizhanovskii, D. M. Whittaker, R. Bouchekioua, D. Sanvitto, S. A. Rizeiqi, R. Bradley, M. S. Skolnick, P. R. Eastham, R. Andre, and L. S. Dang, Physical Review Letters **101**, 067404 (2008).

[32] G. Roumpos, W. H. Nitsche, S. Höfling, A. Forchel, and Y. Yamamoto, Physical Review Letters **104**, 126403 (2010).

[33] H. Deng, G. Weihs, D. Snoke, J. Bloch, and Y. Yamamoto, Proceedings of the National Academy of Sciences of the United States of America **100**, 15318 (2003).

[34] S. Christopoulos, G. B. H. von Hgersthal, A. J. D. Grundy, P. G. Lagoudakis, A. V. Kavokin, J. J. Baumberg, G. Christmann, R. Butt, E. Feltin, J.-F. Carlin, and N. Grandjean, Physical Review Letters **98**, 126405 (2007).

[35] S. Kena-Cohen and S. R. Forrest, Nat Photon **4**, 371 (2010).

[36] A. Das, J. Heo, M. Jankowski, W. Guo, L. Zhang, H. Deng, and P. Bhattacharya, Phys. Rev. Lett. **107**, 066405 (2011).

[37] T.-C. Lu, Y.-Y. Lai, Y.-P. Lan, S.-W. Huang, J.-R. Chen, Y.-C. Wu, W.-F. Hsieh, and H. Deng, Optics Express **20**, 5530 (2012).

[38] T. C. H. Liew and V. Savona, Physical Review Letters **104**, 183601 (2010).

[39] M. Hartmann, F. Brando, and M. Plenio, Laser & Photonics Review **2**, 527 (2008).

FIGURES

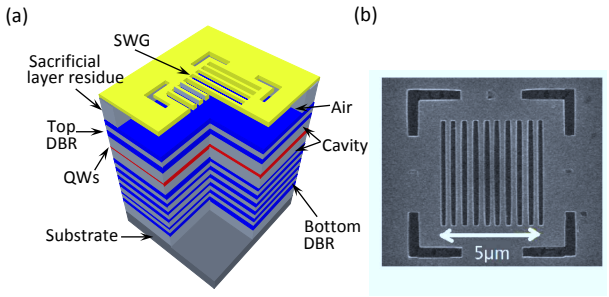

FIG. 1. (color online). (a) A schematic of an example of a 0D hybrid cavity with a SWG mirror. (b) The top-view SEM image of a fabricated 0D cavity with a SWG of 5 μm×5 μm in size.

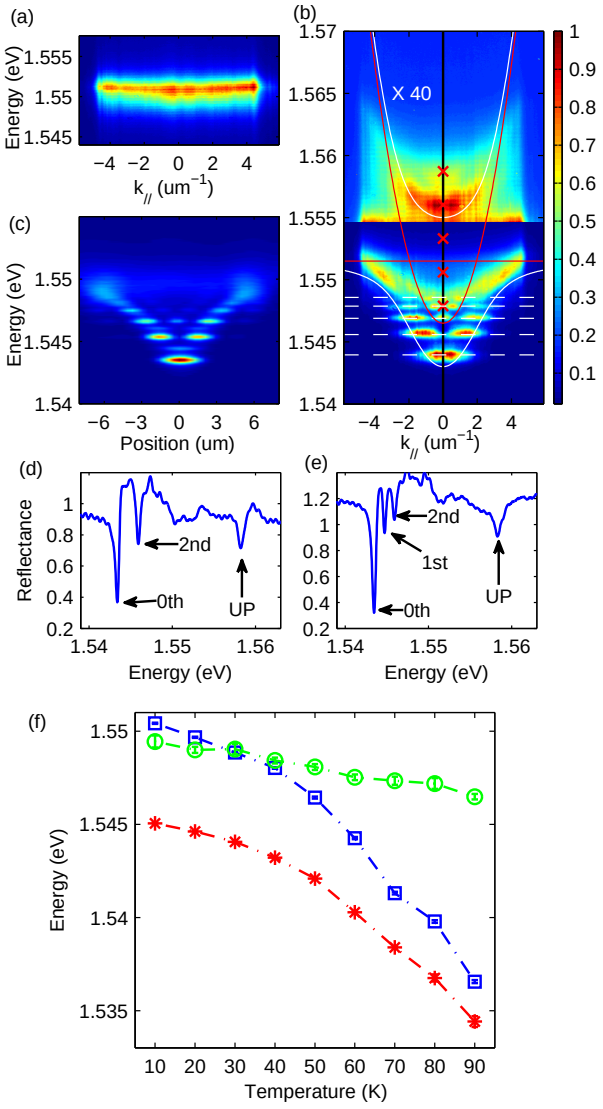
(a)
(b)
(c)
(d)
(e)
(f)
Energy (eV)
k// (um−1)
X 40
Position (um)
Reflectance
2nd
0th
UP
1st
Temperature (K)

FIG. 2. (color online). Spectral properties of a 0D-polariton device. (a) The spectrally resolved momentum space images of the exciton PL, measured from the un-processed part next to the SWG-cavity. (b) The spectrally resolved momentum space image of the PL from a 0D cavity, which shows discrete LP modes and an UP mode. To show clearly the UP mode, the intensity of the upper panel is magnified by 40× compared to the lower panel. The straight red line at 1.551 eV corresponds to the independently measured exciton energy. The other solid lines are the calculated dispersions of the LP, UP and un-coupled cavity. The white dashed lines and the crosses mark the position of the calculated discrete LP and cavity energies, respectively. (c) The spectrally resolved real space image of the PL from the 0D cavity, showing the spatial profile of the discrete LP modes. (d)-(e) Reflectance spectra of the 0D cavity measured from (d) normal direction and (e) from 3.5° from normal direction, both with an angular resolution of 0.27°. (f) Temperature dependence of the LP (red star), exciton (blue square), and cavity resonances (green circle).

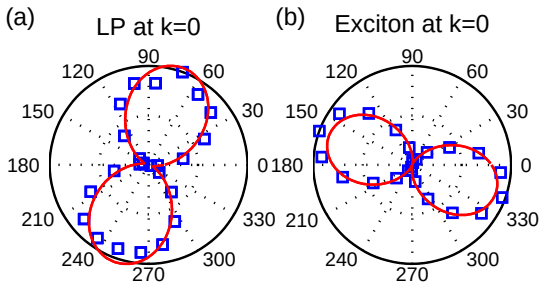

FIG. 3. (color online). Polar plots of the LP (left) and exciton (right) ground state intensities as a function of the angle of the linear polarization analyzer. The symbols are the data. The solid lines are fitting using Eq. 3, which confirms that LP and excitons are orthogonally polarized with the measured linear degrees of polarization of 91.9% and 98.2%, respectively.

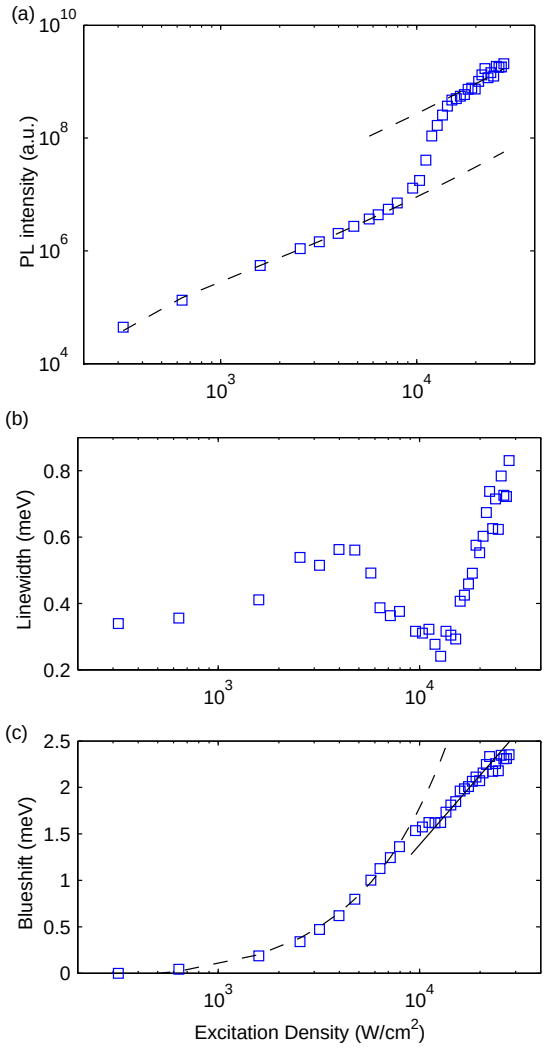

FIG. 4. Lasing properties of the 0D-polaritons. (a) Integrated intensity, (b) linewidth and (c) corresponding energy blue shift of the LP ground state v.s. the excitation density. The dashed lines in (a) are a comparison with quadratic dependence. The dashed lines in (c) are comparisons with the linear dependence below threshold and logarithmic dependence above threshold, respectively.